Hindawi Publishing Corporation
Journal of Nanoparticles
Volume 2013, Article ID 310809, 7 pages
http://dx.doi.org/10.1155/2013/310809

Research Article

Photocatalytic Properties of Microwave-Synthesized TiO_2 and ZnO Nanoparticles Using Malachite Green Dye

A. K. Singh[1,2] and Umesh T. Nakate[1]

[1] *Nanomaterials and Sensors Laboratory, Defence Institute of Advanced Technology, Girinagar, Pune, Maharashtra 411025, India*
[2] *DRDO Centre for Piezoceramics and Devices, ARDE, Pashan, Pune, Maharashtra 411021, India*

Correspondence should be addressed to A. K. Singh; aksingh@diat.ac.in

Received 11 January 2013; Accepted 17 January 2013

Academic Editor: Amir Kajbafvala

TiO_2 and ZnO nanoparticles (NPs) were synthesized using microwave-assisted method. Synthesized NPs were characterized for their structure, morphology, and elemental composition using X-ray diffraction (XRD), scanning electron microscopy (SEM), and energy dispersive spectroscopy (EDS). The crystallite size of synthesized NPs of TiO_2 and ZnO was about 12.3 and 18.7 nm as obtained from the Scherrer formula from the most intense XRD peak. The synthesized NPs have been found to be in stoichiometric ratio having anatase and hexagonal wurtzite structure for TiO_2 and ZnO, respectively, and are spherical in shape. Surface area of TiO_2 and ZnO NPs was found to be about 43.52 m^2/g and 7.7 m^2/g. Photocatalytic (PC) properties of synthesized NPs were studied for malachite green (MG) dye under UV light. TiO_2 NPs were found to be highly photocatalytically active among the two, having efficiency and apparent photodegradation rate of 49.35% and 1.32×10^{-2}, respectively.

1. Introduction

Nowadays, organic pollutants like dyes are becoming a serious health problem, which are being discharged by many industries and houses through wastewater in the environment. The discharged wastes containing dyes are toxic to microorganisms and aquatic life [1]. Malachite green (MG) dye is an extensively used biocide in the global aquaculture industry. It is also used as a food colouring agent, food additive, medical disinfectant, and anthelmintic as well as in silk, wool, jute, leather, cotton, paper, and acrylic industries. However, MG has now become a highly controversial compound due to the risks it poses to the consumers of treated fish, including its effects on the immune system and reproductive system and its genotoxic and carcinogenic properties [2]. In the light of the basic and applied researches reviewed, PC oxidation method appears to be a promising route for the treatment of wastewater contaminated with phenols and dyes. In recent years, there has been a wide research interest in developing semiconductor photocatalysts having high PC activities for environmental applications such as water disinfection, hazardous waste remediation, and water purification [3–5]. It is reported that nanosize semiconductors act as an efficient PC agent resulting from either an extremely large-surface-area-to-volume ratio or quantum confinement effects of charge carriers for the degradation of organic pollutants in water under UV irradiation [6–10]. PC function is similar to the chlorophyll in the photosynthesis. In a PC system, photo-induced molecular transformation or reaction takes place at the surface of the catalyst. A basic mechanism of PC reaction on the generation of electron-hole pair and its destination is as follows: when a photocatalyst is illuminated by the light stronger than its bandgap energy, electron-hole pairs diffuse out to the surface of the PCs and participate in the chemical reaction with the electron donor and acceptor. Those free electrons and holes transform the surrounding oxygen or water molecules into OH free radicals with super strong oxidization [11]. One of the major problems in the PC process is the electron-hole recombination. To avoid this problem, UV irradiation source stands up among other sources [12] because the energy of the UV irradiation is large compared to the bandgap energy of the catalysts. The problem of electron-hole recombination is not fully solved but largely avoided with the use of UV source.

Many photocatalysts like TiO_2, ZnO, ZrO_2, CeO_2, Fe_2O_3, CdS, and ZnS have been attempted for the PC degradation of a wide variety of environmental contaminants. TiO_2 [7] is one of the most widely used semiconductors for PC degradation of waste due to its biological and chemical inertness, high photoreactivity, nontoxicity, and photostability. It is proven that among the three crystalline polymorphs of TiO_2, that is, rutile, anatase, and brookite, the anatase phase or the mixed anatase/rutile phase exhibits better PC properties. The anatase form of TiO_2 has the desirable properties of being chemically stable, readily available, and active as a catalyst for oxidation processes. Bandgap of about 3.2 eV matches the output of a wide variety of readily available lamps. Recently, ZnO [13–17] has also been reported for PC activity having bandgap close to TiO_2. However, only a handful of studies have been attempted which compare the efficiency of different catalysts for a particular organic compound under identical experimental conditions. Serpone and Pelizzetti [18] have reported that TiO_2 and ZnO are the two most active catalysts.

During the recent past, ZnO and TiO_2 were the most widely investigated [19, 20] semiconductors. There are several reported methods of NPs synthesis such as sol-gel [21], organometallic [22], hydrothermal [23, 24], and microwave methods [25–27]. Due to the intense friction and the collision of molecules created by microwave irradiation, microwave irradiation not only provides the energy for heating but also greatly accelerates the nucleation. With microwave irradiation on the reactant solution, temperature and concentration gradients can be avoided leading to uniform nucleation. Microwave-based synthesis method is one of the easiest, energy-saving, green, and quick methods for large-scale production of nanomaterials. Microwave synthesis is the novel route of synthesis of metal oxide semiconductor NPs which is a clean, cost-effective, energy-efficient, eco-friendly, rapid, and convenient method of heating and results in higher yields in shorter reaction times [26, 27].

In the present work, TiO_2 and ZnO NPs were synthesized using the microwave method. These NPs were characterized using XRD, SEM, and EDS. The PC activity of these NPs was studied for MG dye under UV light.

2. Experimental

2.1. Synthesis. For the synthesis of TiO_2, 0.5 M titanium butoxide solution was prepared in 100 mL butanol and stirred for 15 min; further 30 mL deionized water was added dropwise in the above solution to allow hydrolysis. This solution was stirred for 30 min which gave rise to white precipitation. The obtained white precipitate was microwave irradiated for 5 min at 700 W power using Raga's microwave system. The microwave used for this experiment was having a power range of 140 W to 700 W. This obtained solution was left 24 hr for aging at room temperature and then centrifuged at 2000 rpm for 15 min. Obtained precipitate was dried at 80°C for 12 hrs. After complete drying, powder was crushed and calcinated in air at 500°C for 2 hr to remove hydroxide impurities and recrystallization.

For the synthesis of ZnO, NaOH (0.4 M), and zinc acetate (0.2 M), solutions were mixed slowly with molar ratio of 2 : 1, respectively. The above solution was stirred for 10 min. After that, a small quantity of tea was added, and stirring continued for another 10 min. This solution was put for microwave irradiation at 700 W in two steps, that is, 40°C for 20 min and 60°C for 30 min. Resulting precipitate was washed with DI water 2-3 times before drying at 70°C for 4 hr, then crushed using mortar pestle, and calcinated in air at 500°C for 1 hr.

2.2. Characterization. The prepared samples were characterized for their structure, morphology, and elemental composition using X-ray diffraction (XRD) analysis, scanning electron micrograph (SEM), and energy dispersive spectrometry (EDS), respectively. XRD was performed using Bruker AXS, Germany (Model D8 Advanced), diffractometer in the scanning range of 20–70° (2θ) using Cu Ka radiations of wavelength 1.5406 Å. A JEOL ASM 6360A SEM was used to study the morphology and elemental analysis of the NPs. Measurement of BET surface area was carried out for nitrogen adsorption using a Micromeritrics Ins., USA.

2.3. Photocatalytic Activity. Synthesized NPs were used for the photodegradation of MG dye, chemical formula: $[C_6H_5C(C_6H_4N(CH_3)_2)_2]$Cl-4, IUPAC name: [(4-dimethylaminophenyl)phenyl-methyl]-*N,N*-dimethylaniline, under UV light. In each experiment, 40 mL of MG solution of 0.025 g mL^{-1} concentration and 0.005 gr of catalyst were used. This solution was stirred for 10 minutes in the dark for equilibrium of adsorption and desorption process of MG with NPs. After stirring, the solution was irradiated by UV lamp (DYMAX Corporation) under medium intensity spot lamp. The UV lamp was having radiation wavelength range of 200 nm–600 nm with nominal intensity 1000–2000 mW/cm^2. The intensity of absorption peaks, and peak absorbance of NPs was examined by an Ocean Optics UV-Vis high-resolution spectrophotometer (Ocean Optics HR 4000). From which concentrations of MG solution initially and after every 4 minutes of irradiation of UV light were measured from the Lambert–Beer Law [28] that is the absorbance (A) of MG solution is proportional to its concentration (c), which generally followed the following equation:

$$A = \varepsilon bc, \tag{1}$$

where ε is the molar absorption coefficient, and b is the thickness of the absorption cell. In our experiment, all the testing parameters were kept constant, so that ε and b could be considered constant. Therefore, changes in the concentration of MB aqueous solution can be determined by a UV-Vis spectrophotometer.

3. Results and Discussion

3.1. X-Ray Diffraction (XRD). XRD spectra of calcinated samples of TiO_2 and ZnO are shown in Figures 1(a) and 1(b). The obtained diffraction pattern has been compared with JCPDS datasheet JCPDS-080-0074 and JCPDS-84-1284, respectively. From Figures 1(a) and 1(b), it is confirmed from the XRD spectra that the given phase of TiO_2 and ZnO is anatase and hexagonal wurtzite, respectively. The crystallite

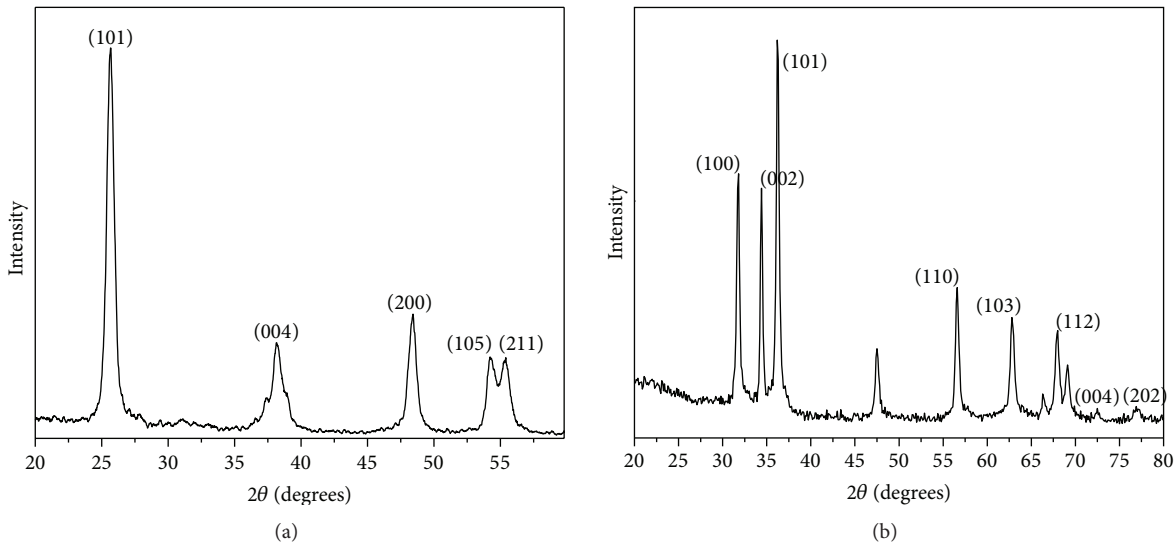

Figure 1: XRD of microwave-synthesized NPs: (a) TiO_2 and (b) ZnO.

Table 1: PC degradation of MG dye performance parameters of all the samples.

Sample	Crystallite size (nm)	K_{app} ($\times 10^{-2}$)	$X_{(32\ min)}$ (%)
TiO_2	12.3	1.32	49.35
ZnO	18.7	0.84	23.31

size, D, of NPs has been calculated by XRD line broadening of the most intense peak using the Scherrer formula [29]

$$D = \frac{K\lambda}{\beta \operatorname{Cos}\theta}, \tag{2}$$

where λ is the wavelength of X-ray, β is the full width and half maxima, θ is Bragg's angle, and K is the shape factor. The dimensionless shape factor has a typical value of about 0.9 but varies with the actual shape of the crystallite. Here, K is taken as 0.9. Crystallite sizes for these NPs are about 12.3 nm and 18.7 nm for TiO_2 and ZnO, respectively, calculated from the most intense peak and shown in Table 1. The sharpness of peaks shows that TiO_2 NPs are highly crystalline in nature.

3.2. Morphology and Elemental Analysis. Morphology of synthesized NPs was studied using scanning electron microscope (SEM) and is shown in Figures 2(a), 2(b), 2(c), and 2(d) at two different magnifications for TiO_2 and ZnO, respectively. Synthesized NPs of TiO_2 and ZnO were found to be spherical in shape, and ZnO NPs are of lower size than TiO_2 with size uniformity. Some agglomeration was also observed in the SEM image of TiO_2, which may be due to calcination NPs. The measured BET surface area of TiO_2 and ZnO NPs has been found to be, respectively, 43.52 m^2/g and 7.7 m^2/g. Elemental analysis of NPs was done by using energy dispersive spectrometer (EDS); the plot of spectrum is shown in Figures 3(a) and 3(b), for TiO_2 and ZnO, respectively. For TiO_2 and ZnO, respectively, the at% of elements detected from EDX is Ti, and O is 54.29 and 45.71; Zn and O are 43.09 and 56.91, respectively, which shows that synthesized NPs are in stoichiometric ratio. The peaks of the plot show the presence of titanium and oxygen elements, zinc and oxygen elements in the corresponding images, that is, Figures 3(a) and 3(b), respectively.

3.3. Photocatalytic Activity. The UV-visible absorbance spectra for photodegradation of MG dye using TiO_2 and ZnO are shown in Figures 4(a) and 4(b), respectively, and corresponding UV-visible spectra of TiO_2 and ZnO are shown in Figure 5. From the plot, it is observed that as irradiation time increases, the concentration of MG dye decreases, which is shown by the decrease in UV-absorbance spectra. The absorption of photon leads to charge separation due to promotion of an electron (e^-) from the valence band of the semiconductor catalyst to the conduction band, thus generating a hole (h^+) in the valence band. Light source provides photon energy required to excite the semiconductor electron from the valence band (VB) region to the conduction band (CB) region. With the increase in irradiation having sufficient intensity, photodegradation efficiency increases because electron-hole formation is predominantly increasing, and electron-hole recombination is negligible at sufficiently higher intensity, whereas at lower light intensity, electron-hole pair separation competes with recombination which in turn decreases the formation of free radicals, thereby, causing less effect on the percentage degradation of the dyes.

Mechanism for photodegradation of MG dye can be explained as follows. On illumination of catalyst surface with enough energy (equals or higher than the bandgap energy, E_{bg}, of the catalyst), it leads to the formation of a hole (h^+) in the valence band and an electron (e^-) in the conduction band. The hole oxidizes either pollutant directly or water to produce OH^- radicals, whereas the electron in the conduction band reduces the oxygen adsorbed on the catalyst. The activation

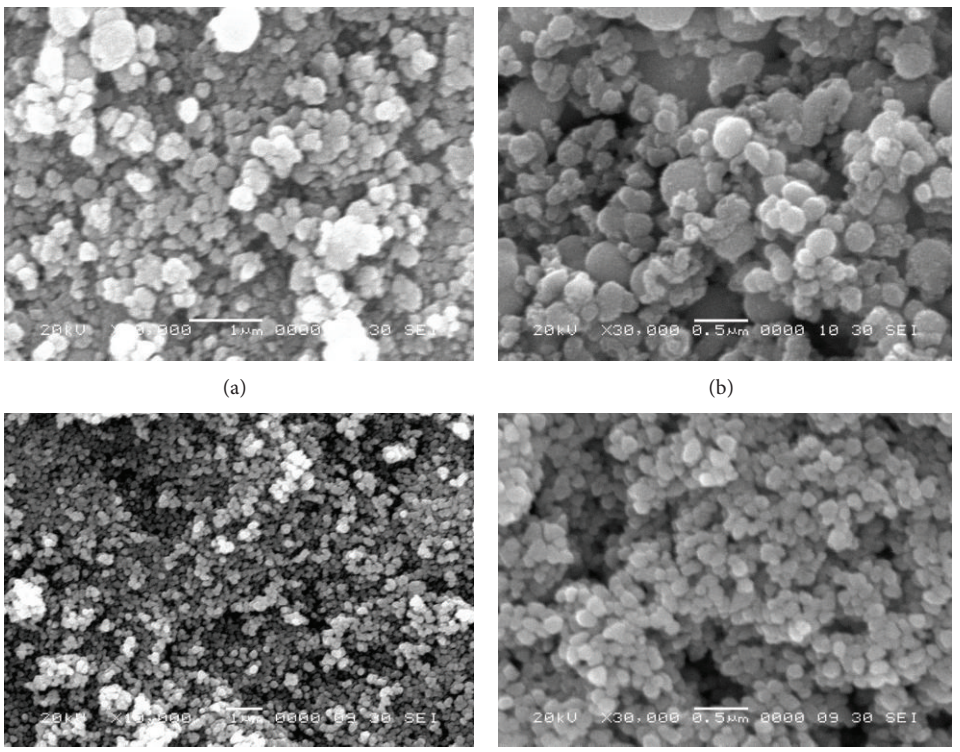

(a) (b) (c) (d)

Figure 2: SEM image of microwave-synthesized NPs at different magnifications: (a)-(b) for TiO_2 and (c)-(d) for ZnO NPs.

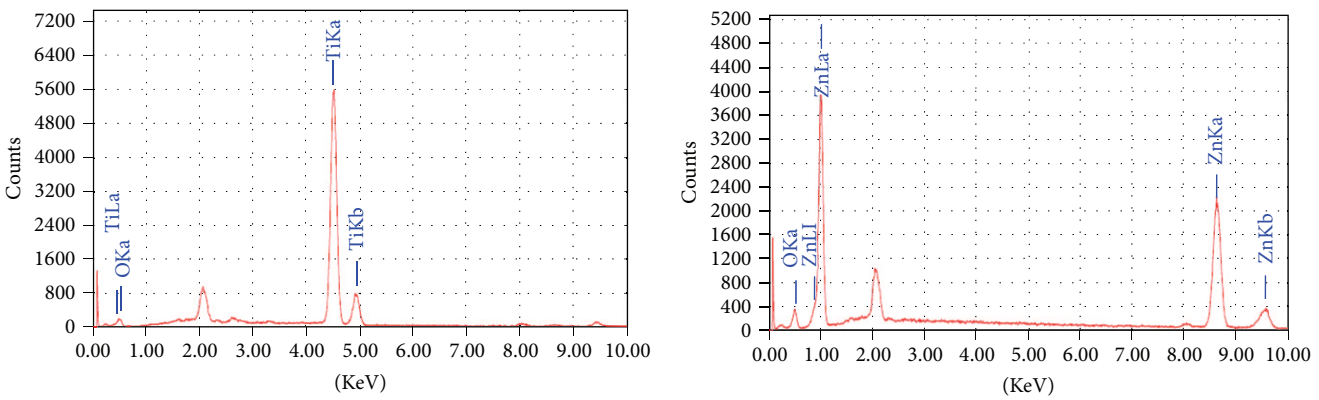

(a) (b)

Figure 3: EDS spectrum of microwave-synthesized samples: (a) TiO_2 and (b) ZnO NPs.

of catalyst (TiO_2 or ZnO) by UV light can be represented by the following steps:

$$\text{Catalyst} + h\nu \longrightarrow e^- + h^+ \quad (3)$$

$$e^- + O_2 \longrightarrow O_2^- \quad (4)$$

In this reaction, h^+ and e^- are powerful oxidizing and reductive agents, respectively. The oxidative and reductive reaction steps are expressed as follows:

$$h^+ + \text{MG} \longrightarrow \text{degradation compounds} \quad (5)$$

$$h^+ + H_2O \longrightarrow OH^- + H^+ \quad (6)$$

$$OH^- + \text{MG} \longrightarrow \text{degradation compounds} \quad (7)$$

One of the major problems in the photocatalytic process is the electron-hole recombination. To avoid this problem, UV irradiation source stands up among other sources [12]. The energy of UV irradiation is large compared to the bandgap energy of the catalysts. Hence, the problem of electron-hole recombination is not fully but largely avoided with UV

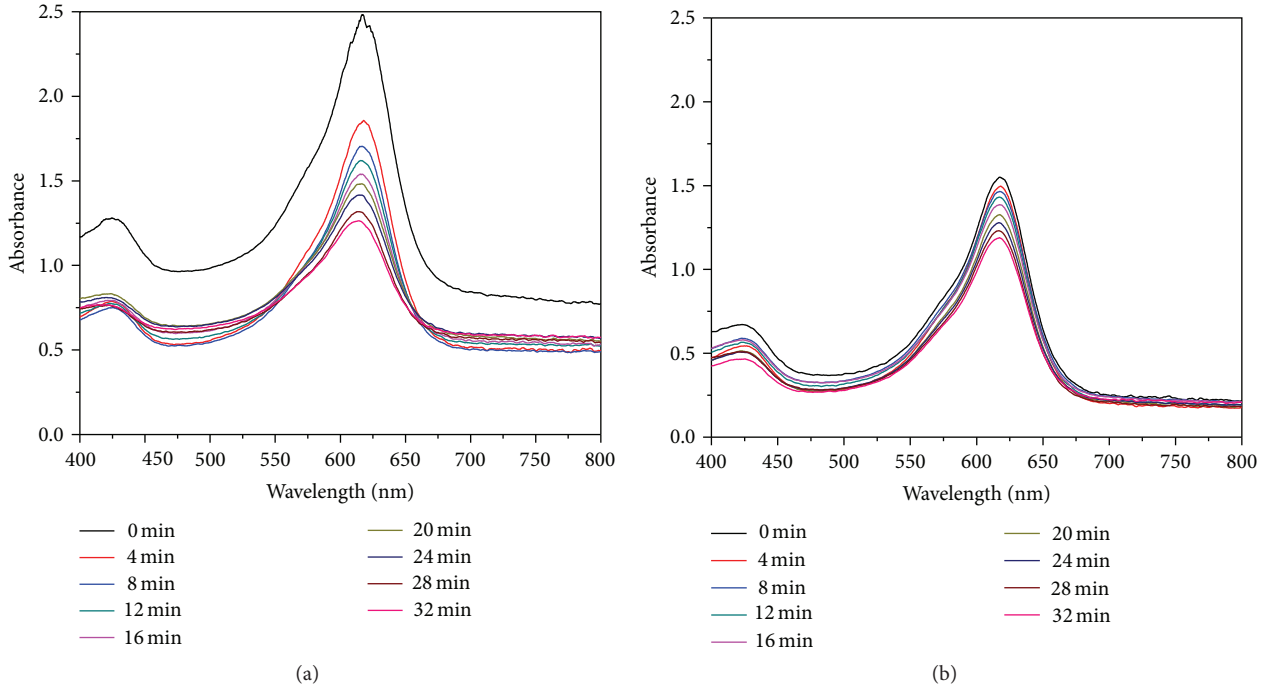

Figure 4: UV absorbance spectra of catalyst during photodegradation of MG dye for (a) TiO_2 NPs and (b) ZnO NPs.

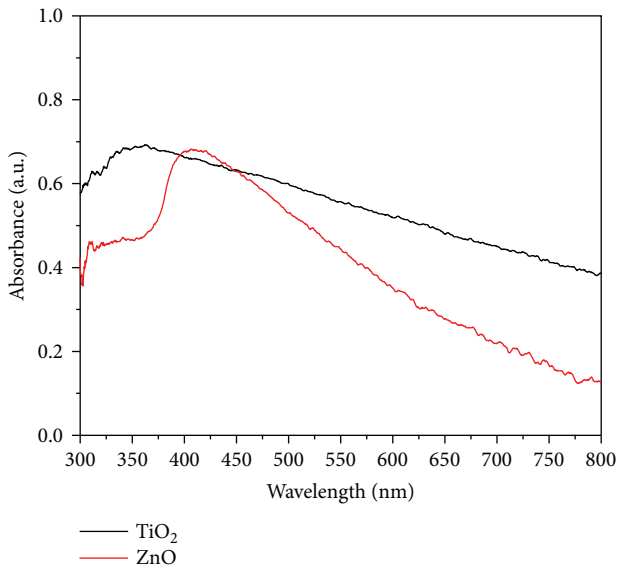

Figure 5: UV absorbance spectra of synthesized TiO_2 NPs and ZnO NPs.

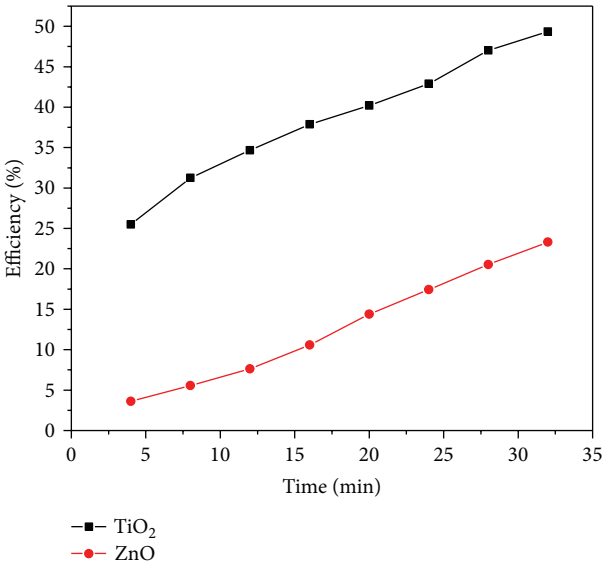

Figure 6: Photodegradation percentage efficiency for TiO_2 and ZnO catalysts.

source. The percentage efficiency of photodegradation was determined using the following equation [30]:

$$X = \frac{C_o - C}{C_o} \times 100, \tag{8}$$

where C_0 is the initial solution concentration of MG and C is the solution concentration of MG after degradation. The graph of percentage efficiency with irradiation time is shown in Figure 6. It is clear from the figure that as irradiation time increases the efficiency of nanoparticles to degrade MG dye also increases. Here, TiO_2 NPs are found to be more efficient catalysts than ZnO NPs. The apparent rate constant for degradation of MG was determined using the following equation [30]:

$$\ln\left(\frac{C_0}{C}\right) = K_{\text{app}}t. \tag{9}$$

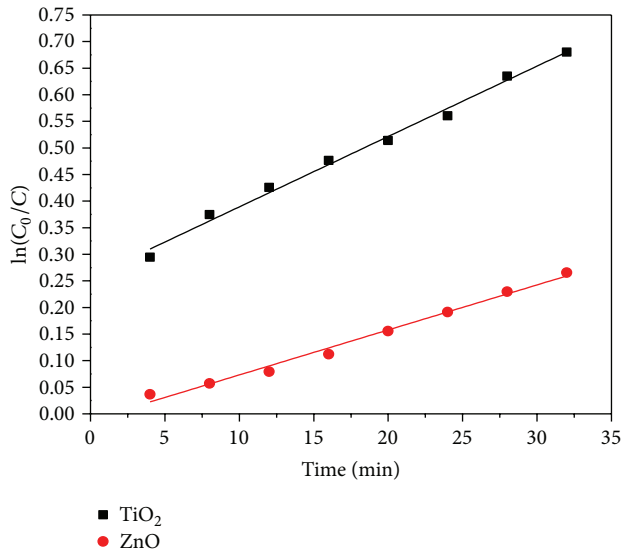

FIGURE 7: Apparent rate constant for degradation of MG dye by synthesized TiO_2 and ZnO NPs catalysts.

K_{app} (min^{-1}) is the observed first-order rate constant. In the early stage of the reaction (i.e., up to 30 min), MG degradation is found to follow first-order kinetics according to the equation. This empirical equation has been used from common first-order kinetics and proposed for the simple description of the decay process [31]. The plot of ln (C_0/C) with irradiation time is shown in Figure 7 where the slopes represent the apparent rate constant for degradation of MG dye. The apparent rate constants of TiO_2 and ZnO catalysts are given in Table 1. Here, we found that TiO_2 NPs have higher apparent rate constant than other ZnO NPs; this is due to TiO_2 having wide bandgap and highly sensitivity to UV radiations, as can be seen in Figure 5. The bandgap value of anatase TiO_2 is around 3.2 eV, which enables UV light of wavelengths smaller than 400 nm to activate the catalyst [32].

4. Conclusions

In this study, synthesis of uniform size TiO_2 and ZnO nanoparticles was achieved using microwave synthesis which is considered to be a green, efficient, and cost-effective method having potential for large-scale synthesis. Photocatalytic properties of synthesized TiO_2 and ZnO nanoparticles were studied which shows that TiO_2 and ZnO nanoparticles have 49.35% and 23.31% photodegradation efficiency, respectively, for MG dye under UV light. TiO_2 nanoparticles show more than two-order photodegradation property for MG dye as compared to ZnO.

Acknowledgments

The authors are thankful to the director of ARDE, Pashan, Pune, for granting permission to publish this work. Thanks are also due to the Department of Physics, University of Pune, for SEM and XRD of samples.

References

[1] P. Borker and A. V. Salker, "Photocatalytic degradation of textile azo dye over $Ce_{1-x}Sn_xO_2$ series," *Materials Science and Engineering B*, vol. 133, pp. 55–60, 2006.

[2] C. C. Chen, C. S. Lu, Y. C. Chung, and J. L. Jan, "UV light induced photodegradation of malachite green on TiO_2 nanoparticles," *Journal of Hazardous Materials*, vol. 141, no. 3, pp. 520–528, 2007.

[3] A. Fujishima, T. N. Rao, and D. A. Tryk, "Titanium dioxide photocatalysis," *Journal of Photochemistry and Photobiology C*, vol. 1, pp. 1–21, 2000.

[4] C. Kormann, D. W. Bahnemann, and M. R. Hoffmann, "Photolysis of chloroform and other organic molecules in aqueous TiO_2 suspensions," *Environmental Science and Technology*, vol. 25, no. 3, pp. 494–500, 1991.

[5] J. Peral and D. F. Ollis, "Heterogeneous photocatalytic oxidation of gas-phase organics for air purification: acetone, 1-butanol, butyraldehyde, formaldehyde, and m-xylene oxidation," *Journal of Catalysis*, vol. 136, no. 2, pp. 554–565, 1992.

[6] S. Chakrabarti and B. K. Dutta, "Photocatalytic degradation of model textile dyes in waste water using ZnO as semiconductor catalyst," *Journal of Hazardous Materials B*, vol. 112, pp. 269–278, 2004.

[7] G. P. Fotou and S. E. Pratsinis, "Photocatalytic destruction of phenol and salicylic acid with aerosol-made and commercial titania powders," *Chemical Engineering Communications*, vol. 151, pp. 251–269, 1996.

[8] M. L. Curridal, R. Comparelli, P. D. Cozzli, G. Mascolo, and A. Agostiano, "Colloidal oxide nanoparticles for the photocatalytic degradation of organic dye," *Materials Science and Engineering C*, vol. 23, no. 1-2, pp. 285–289, 2003.

[9] S. B. Park and Y. C. Kang, "Photocatalytic activity of nanometer size ZnO particles prepared by spray pyrolysis," *Journal of Aerosol Science*, vol. 28, pp. S473–S474, 1997.

[10] R. Y. Hong, T. T. Pan, J. Z. Qian, and H. Z. Li, "Synthesis and surface modification of ZnO nanoparticles," *Chemical Engineering Journal*, vol. 119, no. 2-3, pp. 71–81, 2006.

[11] Y. J. Jang, C. Simer, and T. Ohm, "Comparison of zinc oxide nanoparticles and its nano-crystalline particles on the photocatalytic degradation of methylene blue," *Materials Research Bulletin*, vol. 41, no. 1, pp. 67–77, 2006.

[12] B. Neppolian, H. C. Choi, S. Sakthivel, B. Arabindoo, and V. Murugesan, "Solar/UV-induced photocatalytic degradation of three commercial textile dyes," *Journal of Hazardous Materials B*, vol. 89, no. 2-3, pp. 303–317, 2002.

[13] Y. Zhang, F. Zhu, J. Zhang, and L. Xia, "Converting layered zinc acetate nanobelts to one-dimensional structured ZnO nanoparticle aggregates and their photocatalytic activity," *Nanoscale Research Letters*, vol. 3, no. 6, pp. 201–204, 2008.

[14] M. Zhang, G. Sheng, J. Fu, T. An, X. Wang, and X. Hu, "Novel preparation of nanosized ZnO–SnO_2 with high photocatalytic activity by homogeneous co-precipitation method," *Materials Letters*, vol. 59, no. 28, pp. 3641–3644, 2005.

[15] C. Wang, X. Wang, B. Q. Xu et al., "Enhanced photocatalytic performance of nanosized coupled ZnO/SnO_2 photocatalysts for methyl orange degradation," *Journal of Photochemistry and Photobiology A*, vol. 168, no. 1-2, pp. 47–52, 2004.

[16] W. Cun, Z. Jincai, W. Xinming et al., "Preparation, characterization and photocatalytic activity of nano-sized ZnO/SnO_2 coupled photocatalysts," *Applied Catalysis B*, vol. 39, no. 3, pp. 269–279, 2002.

[17] A. Kajbafvala, H. Ghorbani, A. Paravar, J. P. Samberg, E. Kajbafvala, and S. K. Sadrnezhaad, "Effects of morphology on photocatalytic performance of Zinc oxide nanostructures synthesized by rapid microwave irradiation methods," *Superlattices and Microstructures*, vol. 51, no. 4, pp. 512–522, 2012.

[18] N. Serpone and E. Pelizzetti, Eds., *Photocatalysis: Fundamentals and Applications*, Wiley, New York, NY, USA, 1989.

[19] A. K. Singh, "Synthesis, characterization, electrical and sensing properties of ZnO nanoparticles," *Advanced Powder Technology*, vol. 21, pp. 609–613, 2010.

[20] J. Wang, J. Polleux, J. Lim, and B. Dunn, "Pseudocapacitive contributions to electrochemical energy storage in TiO_2 (anatase) nanoparticles," *Journal of Physical Chemistry C*, vol. 111, no. 40, pp. 14925–14931, 2007.

[21] T. Sugimoto, X. Zhou, and A. Muramatsu, "Synthesis of uniform anatase TiO_2 nanoparticles by gel-sol method: 3. Formation process and size control," *Journal of Colloid and Interface Science*, vol. 259, no. 1, pp. 43–52, 2003.

[22] J. Tang, F. Redl, Y. Zhu, T. Siegrist, L. E. Brus, and M. L. Steigerwald, "An organometallic synthesis of TiO_2 nanoparticles," *Nano Letters*, vol. 5, no. 3, pp. 543–548, 2005.

[23] S. Jeon and P. V. Braun, "Hydrothermal synthesis of Er-doped luminescent TiO_2 nanoparticles," *Chemistry of Materials*, vol. 15, no. 6, pp. 1256–1263, 2003.

[24] S. K. Sahoo, M. Mohapatra, A. K. Singh, and S. Anand, "Hydrothermal synthesis of single crystalline nano CeO_2 and its structural, optical, and electronic characterization," *Materials and Manufacturing Processes*, vol. 25, no. 9, pp. 982–989, 2010.

[25] A. K. Singh, "Microwave synthesis, optical, structural and magnetic properties of ZnO/Mn doped ZnO nanostructures," *Journal of Optoelectronics and Advanced Materials*, vol. 12, pp. 2255–2260, 2010.

[26] P. Periyat, N. Leyland, D. E. McCormack, J. Colreavy, D. Corr, and S. C. Pillai, "Rapid microwave synthesis of mesoporous TiO_2 for electrochromic displays," *Journal of Materials Chemistry*, vol. 20, no. 18, pp. 3650–3655, 2010.

[27] A. Kajbafvala, J. P. Samberg, H. Ghorbani, E. Kajbafvala, and S. K. Sadrnezhaad, "Effects of initial precursor and microwave irradiation on step-by-step synthesis of zinc oxide nanoarchitectures," *Materials Letters*, vol. 67, no. 1, pp. 342–345, 2012.

[28] H. Kumazawa, M. Inoue, and T. Kasuya, "Photocatalytic degradation of volatile and nonvolatile organic compounds on titanium dioxide particles using fluidized beds," *Industrial and Engineering Chemistry Research*, vol. 42, no. 14, pp. 3237–3244, 2003.

[29] P. B. Bagdare, S. B. Patil, and A. K. Singh, "Phase evolution and PEC performance of $Zn_xCd_{(1-x)}S$ nanocrystalline thin films deposited by CBD," *Journal of Alloys and Compounds*, vol. 506, no. 1, pp. 120–124, 2010.

[30] S. Ghasemi, S. Rahimnejad, S. Rahman Setayesh, S. Rohani, and M. R. Gholami, "Transition metal ions effect on the properties and photocatalytic activity of nanocrystalline TiO_2 prepared in an ionic liquid," *Journal of Hazardous Materials*, vol. 172, no. 2-3, pp. 1573–1578, 2009.

[31] G. Mascolo, R. Comparelli, M. L. Curri, G. Lovecchio, A. Lopez, and A. Agostiano, "Photocatalytic degradation of methyl red by TiO_2: comparison of the efficiency of immobilized nanoparticles versus conventional suspended catalyst," *Journal of Hazardous Materials*, vol. 142, no. 1-2, pp. 130–137, 2007.

[32] A. H. C. Chan, C. K. Chan, J. P. Barford, and J. F. Porter, "Solar photocatalytic thin film cascade reactor for treatment of benzoic acid containing wastewater," *Water Research*, vol. 37, no. 5, pp. 1125–1135, 2003.